On the Feasibility of Time-Modulated Arrays for Digital Linear Modulations: A Theoretical Analysis

Roberto Maneiro-Catoira, Julio Brégains, *Senior Member, IEEE,*
José A. García-Naya, *Member, IEEE,* and Luis Castedo, *Member, IEEE*

Abstract

Wireless communications are widely based on linear digital modulation methods, which introduce the digital baseband information in the amplitude and/or in the phase of a carrier sinusoid. Time-modulated arrays, on the other hand, constitute an interesting technique capable of adapting the power radiation pattern of an antenna array. In this work we study, from a theoretical point of view, the impact of time-modulated arrays on the transmission of linearly modulated digital communication signals. The work focuses on the requirements to safeguard the integrity of the signal and on the quantification of the useful power radiated within the desired band.

Index Terms

Antenna arrays, communication, modulation.

I. Introduction

Time modulation applied to a linear antenna array is a technique to adapt its radiated power pattern by means of periodically enabling and disabling the excitations of the individual array elements [1]. This technique was initially introduced to control the sidelobes level of the power pattern radiated by an antenna array suitable for radar applications. Since the early 2000s there has

The authors are with the Department of Electronics and Systems at the University of A Coruña, 15071 A Coruña, Spain. E-mail:{roberto.maneiro, julio.bregains, jagarcia, luis}@udc.es

been renewed interest in taking up the investigations on this field. In this sense, some optimization algorithms have been recently developed to minimize the Sideband Radiation (SR) [2]–[8]. More recent works [9]–[11] have achieved a major control over the sidelobes of the main power pattern as well as a significant reduction of the SR through the strategic control of the on/off pulses that modulate the excitations of the antenna elements. As the harmonics losses could be relatively high, some works have focused on the calculation of the Time-Modulated Array (TMA) gain and on the calculation of the harmonics power levels [10], [12]–[15]. However, the SR is not necessarily detrimental, and sometimes can be profitably exploited. In fact, some works focus on the potential of TMA as a smart antenna in time-varying scenarios to incorporate features like real-time adaptive nulling [16], adaptive beam forming [17], [18], beam steering [19] or Direction of Arrival (DoA) estimation [20]. In most cases, the analyses do not specify explicitly the target application of the TMA. Since some of the TMA elements are subject to on/off pulse trains, it is understandable to be reticent to think that such a technique could be successfully applied to transmit broadband communication signals. Some authors [12], [21], [22], however, have considered such a possibility, and they have concluded that signal transmission through a TMA is possible under certain restrictions on the involved frequencies [12]. TMA technology has also been proposed to transmit direction-dependent signals in secure communications [23]. In none of the cases, however, an in-depth theoretical study considering the influence of a TMA on a digital communication system was presented, which is precisely the main aim of this work.

Digital modulation is the process of translating bits into analog waveforms suitable for being transmitted over a physical channel. The input bit stream is grouped into blocks of k bits and such blocks are referred to as symbols. For each symbol, a different signal of duration T_s is chosen. Hence, each symbol is mapped into one of $M = 2^k$ different waveforms.

Linear modulation methods in which the transmitted signal depends linearly on the information symbols to be sent are the most widely used forms of digital modulations. In such cases the digital information is coded in the amplitude and/or the phase of a carrier sinusoidal signal. Among the factors influencing the choice of a digital modulation, spectral efficiency (bit rate per bandwidth unit, expressed in bit/s/Hz) and power efficiency are of great importance.

Nonlinear modulations such as Frequency-Shift Keying (FSK) [24] and its variants are power efficient and very robust against both channel impairments and non-linearities. However, they exhibit worse spectral efficiency than their linear counterparts. Linear modulations such as

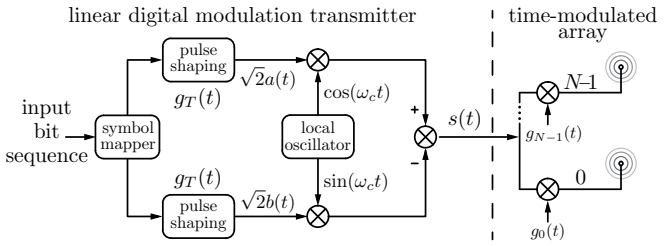

Fig. 1. Transmitter block diagram of the system under study.

Amplitude-Shift Keying (ASK), Phase-Shift Keying (PSK), and Quadrature Amplitude Modulation (QAM) are spectral efficient but not power-efficient by themselves [24]. Nevertheless, when combined with channel coding, linear modulations can also be made power-efficient and this is the reason why they are being used in most of today's wireless communication standards.

ASK modulation presents a poor noise protection as the alphabet size M increases. Both ASK and QAM modulations do not have a constant envelope, so the performance degrades in the presence of non-linearities. PSK overcomes such a limitation because the signal envelope is kept constant.

For high values of M QAM is preferred to PSK. Even though both offer the same spectral efficiency, QAM is more resilient to noise. QAM will be the usual modulation when M is high (i.e. 16, 64, or 256), and for this reason they are usually called high-order modulations [25]. QAM provides both high data rates and high spectral efficiency. Consequently, it is particularly suitable for those applications in which bandwidth is limited and high data rates are demanded, as for example in satellite systems or mobile wireless communications [24]. Apart from the above reasons, linear modulation is one of the simplest schemes to be considered in any analysis pertaining signal transmission systems. Those conditions represent an ideal frame to start with, and it is the one chosen in this work.

By incorporating a TMA (whose primary purpose is to adjust the radiated power pattern) to a radio system based on a linear digital modulation scheme (see Fig. 1) we will show that it is possible to obtain an adequate system performance under certain restrictions. To accurately analyze the control of the power radiation pattern obtained through a TMA when linearly modulated signals are transmitted, we provide a mathematical analysis with two different objectives. First, we determine the TMA restrictions in terms of the parameters of the linearly modulated digital signal to guarantee the integrity of the information transmitted. Second, we

derive an expression for both the total power and the useful power radiated when a linearly modulated signal is transmitted by the TMA. The special motivation for the last objective is to model theoretically the power-radiated efficiency of the TMA when it is combined with digital linear modulation schemes. In other words, we want to know how much of the radiated power is lost because of the TMA.

II. Mathematical Fundamental Analysis

A. Time-Modulated Array Fundamentals

The radiated field of a linear TMA composed of N isotropic elements distributed along the z axis is given by the following expression [12]–[14], [21]

$$F(\theta,t)=\mathrm{e}^{j\omega_c t}\sum_{n=0}^{N-1} g_n(t) I_n \mathrm{e}^{jkz_n\cos\theta}\in\mathbb{C}, \tag{1}$$

where $g_n(t)$ is a periodic function (with period $T_0=2\pi/\omega_0$) usually considered to be a rectangular pulse train governing the n-th switch; $I_n=|I_n|\mathrm{e}^{j\varphi_n}$ and z_n are respectively the complex current excitation in polar form (φ_n is its phase) and the position on the z-axis for the n-th array element; the θ variable corresponds to the angle with respect to the z-axis (notice that, for such an array geometrical configuration, the φ coordinate is not necessary); $k=2\pi/\lambda$ represents the wavenumber for a carrier wavelength $\lambda=2\pi c/\omega_c=c/f_c$; and $\mathbb{C}$ is the set of complex numbers.

Let us consider the Fourier series expansion of the n-th array element modulating pulse:

$$g_n(t)=\sum_{q=-\infty}^{\infty} G_{nq}\mathrm{e}^{jq\omega_0 t}\in\mathbb{R}, \tag{2}$$

being $\omega_0=2\pi/T_0=2\pi f_0$, and $\mathbb{R}$ the set of real numbers.

By substituting (2) in (1) we have:

$$\begin{aligned}F(\theta,t)=&\left[\sum_{n=0}^{N-1} I_n G_{n0}\mathrm{e}^{jkz_n\cos\theta}\right]\mathrm{e}^{j\omega_c t}+\\&+\left[\sum_{n=0}^{N-1}\sum_{\substack{q=-\infty\\q\neq 0}}^{\infty} I_n G_{nq}\mathrm{e}^{jkz_n\cos\theta}\right]\mathrm{e}^{j(\omega_c+q\omega_0)t}.\end{aligned} \tag{3}$$

The first term in (3) is the array factor at ω_c, which allows for controlling the radiated pattern through the G_{n0} coefficients. When $g_n(t)$ is a periodic train of rectangular pulses of duration τ_n

(i.e. the array elements are controlled by on-off switches), then G_{n0} corresponds to the normalized duration $\xi_n = \tau_n/T_0$ [6].

The second term in (3) reveals the presence of harmonics located at frequencies $\omega_c + q\omega_0$, which can be either minimized using TMA optimization techniques [2], [3], [5]–[11], [15] or used profitably [16]–[20]. Note that the G_{nq} coefficients will influence the amplitude level – and thus the topology– of the main pattern ($q = 0$) and also the decay rate of the harmonics (increasing $|q|$ values) levels. In the analyses that follow, we will consider that the G_{nq} lead to relatively fast decaying rates of the harmonics maximum levels as, for example, in those cases of the above-mentioned optimized configurations.

B. Linear Digital Modulation Fundamentals

A generalized linear modulation scheme may be viewed as a system in which the message is inserted in the amplitude $A(t)$ and/or in the phase $\alpha(t)$ of the transmitted signal $s(t) \in \mathbb{R}$ whose carrier frequency is $\omega_c = 2\pi f_c$ (see Fig. 1). Therefore, a linearly modulated signal can be written as

$$s(t) = \sqrt{2}A(t)\cos(\omega_c t + \alpha(t)) = \mathrm{Re}\left\{\sqrt{2}u(t)\mathrm{e}^{j\omega_c t}\right\}, \tag{4}$$

where

$$u(t) = A(t)\mathrm{e}^{j\alpha(t)} = a(t) + jb(t) \in \mathbb{C} \tag{5}$$

is the so-called complex-valued envelope or equivalent baseband signal of $s(t)$, and with

$$a(t) = A(t)\cos(\alpha(t)), \text{ and } b(t) = A(t)\sin(\alpha(t)).$$

The term $\sqrt{2}$ in (4) is included to ensure that the bandpass signal $s(t)$ and the equivalent baseband signal $u(t)$ have the same mean power, as shown in the forthcoming analysis results (see Eqs. (39) and (53)). According to Eqs. (4) and (5), the signal under consideration can also be written as

$$s(t) = \sqrt{2}a(t)\cos(\omega_c t) - \sqrt{2}b(t)\sin(\omega_c t), \text{ with} \tag{6}$$

$$a(t) = \sum_{k=-\infty}^{\infty} a_k g_T(t - kT_s) \text{ and } b(t) = \sum_{k=-\infty}^{\infty} b_k g_T(t - kT_s) \tag{7}$$

being the so-called In-phase (I) and Quadrature (Q) signal components, respectively. The complex numbers $a_k + jb_k$ represent symbols to be transmitted and taken from a constellation mapping;

T_s is the duration (period) of each symbol; and $g_T(t)$ is the transmit pulse-shaping filter being, in our case, a raised cosine shaping filter with roll-off factor ρ [24].

C. Restrictions for Single-Carrier Transmission: Frequency and Time-Domain Analysis

Let us consider that a linearly-modulated digital signal is radiated through a TMA. From Eqs. (1) and (5), the signal radiated by the n-th array element is given by (see Fig. 1)

$$\begin{aligned} s_n(\theta,t) = \sqrt{2}A(t)|I_n|g_n(t)\cdot \\ \cdot \cos\left(\omega_c t + \varphi_n + kz_n\cos\theta + \alpha(t)\right). \end{aligned} \tag{8}$$

In order to simplify the subsequent analysis, let us consider the complex-valued representation of $s_n(t)$ given by

$$\begin{aligned} \tilde{s}_n(\theta,t) &= \left[\sqrt{2}u(t)g_n(t)I_n\mathrm{e}^{jkz_n\cos\theta}\right]\mathrm{e}^{j\omega_c t} \\ &= r_n(\theta,t)\mathrm{e}^{j\omega_c t} \in \mathbb{C}, \end{aligned} \tag{9}$$

where $r_n(\theta,t) = \sqrt{2}u(t)g_n(t)I_n\mathrm{e}^{jkz_n\cos\theta}$ is the complex envelope of the analytic signal $\tilde{s}_n(\theta,t)$.

The signal radiated by the TMA results from the sum of the contributions from all N array elements

$$\begin{aligned} \tilde{s}_{\text{rad}}(\theta,t) &= \sum_{n=0}^{N-1}\tilde{s}_n(\theta,t) \\ &= \left[\sqrt{2}u(t)\sum_{n=0}^{N-1}g_n(t)I_n\mathrm{e}^{jkz_n\cos\theta}\right]\mathrm{e}^{j\omega_c t} \\ &= \sqrt{2}u(t)F(\theta,t), \end{aligned} \tag{10}$$

with $F(\theta,t)$ defined in (1) whereas $\tilde{s}_{\text{rad}}(\theta,t)$ is the analytic representation of the radiated signal. Note now that the Fourier Transform (FT) of $g_n(t) = \sum_{q=-\infty}^{\infty}G_{nq}\mathrm{e}^{jq\omega_0 t}$ is

$$G_n(\omega) = \mathrm{FT}[g_n(t)] = 2\pi\sum_{q=-\infty}^{\infty}G_{nq}\delta(\omega - q\omega_0), \tag{11}$$

which is expressed in terms of the frequency $\omega = 2\pi f$.

On the other hand, according to the FT properties, a multiplication in the time domain corresponds to a convolution (denoted here by $\star$) in the frequency domain, which for two given signals $x(t)$ and $y(t)$ yields

$$\mathrm{FT}\left[x(t)\,y(t)\right] = \frac{1}{2\pi}X(\omega)\star Y(\omega). \tag{12}$$

Applying (12) to $u(t)g_n(t)$, considering the linearity of the FT, and that $U(\omega) = \mathrm{FT}\,[u(t)]$, the FT of $r_n(t)$ is

$$\begin{aligned} R_n(\theta,\omega) &= \mathrm{FT}\,[r_n(\theta,t)] \\ &= \sqrt{2}\sum_{q=-\infty}^{\infty} I_n \mathrm{e}^{jkz_n\cos\theta} G_{nq} U(\omega - q\omega_0). \end{aligned} \tag{13}$$

Now, since $\mathrm{FT}\,[r_n(\theta,t)\mathrm{e}^{j\omega_c t}] = R_n(\theta,\omega-\omega_c)$, considering (13) we obtain

$$\tilde{S}_n(\omega) = \sqrt{2}\sum_{q=-\infty}^{\infty} I_n \mathrm{e}^{jkz_n\cos\theta} G_{nq} U(\omega - (\omega_c + q\omega_0)), \tag{14}$$

and then, the spectrum of $\tilde{s}_{\text{rad}}(t)$ is expressed as

$$\begin{aligned} \tilde{S}_{\text{rad}}(\omega) &= \sum_{n=0}^{N-1} \tilde{S}_n(\omega) \\ &= \sqrt{2}\sum_{n=0}^{N-1}\sum_{q=-\infty}^{\infty} I_n \mathrm{e}^{jkz_n\cos\theta} G_{nq} U(\omega - (\omega_c + q\omega_0)). \end{aligned} \tag{15}$$

By observing (15) we conclude that

1) The desired radiated signal is the one corresponding to $q = 0$ (the so-called fundamental mode) and it is given by:

$$\tilde{S}_{\text{rad}}(\omega)\Big|_{q=0} = \sqrt{2}\sum_{n=0}^{N-1} I_n G_{n0} \mathrm{e}^{jkz_n\cos\theta} U(\omega - \omega_c), \tag{16}$$

with $G_{n0} = \xi_n$ when $g_n(t)$ is a periodic train of rectangular pulses. Equation (16) has the same spectrum topology as if $s(t)$ were radiated through a conventional array but now having control over the dynamic excitations $I_n G_{n0} = I_n \xi_n$.

2) The terms corresponding to $q \neq 0$ are signal replicas centered at the frequencies $\omega_c + q\omega_0$. To avoid interferences between the TMA (carrier at ω_0) and the linearly-modulated digital signal $s(t)$ centered at ω_c, an immediate requirement is mandatory:

$$\omega_0 \ll \omega_c \Leftrightarrow f_0 \ll f_c \Leftrightarrow T_0 \gg 1/f_c \quad \textbf{(restriction 1)}. \tag{17}$$

As the linearly-modulated digital signal has a limited bandwidth B_ω [rad/s], an additional restriction is necessary to avoid overlapping between the signal replicas and the fundamental mode. Figure 2 is a simplified graphical representation of (15), which is helpful for deriving the following condition

$$\omega_c + q\omega_0 - \frac{B_\omega}{2} > \omega_c + \frac{B_\omega}{2} \Rightarrow q\omega_0 > B_\omega. \tag{18}$$

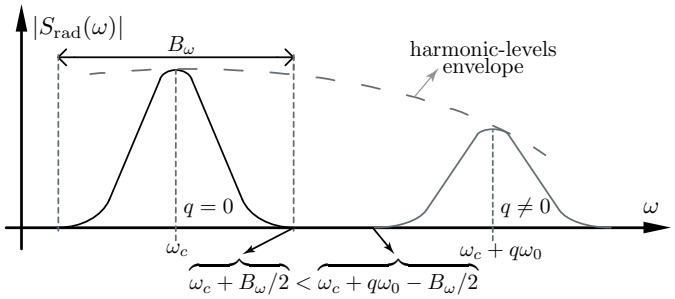

Fig. 2. Non-overlapping condition between the replicas of the transmitted signal and the fundamental mode.

By selecting the closest harmonic to the carrier frequency (i.e. choosing $|q|=1$), the restriction becomes

$$\omega_0 > B_\omega. \tag{19}$$

Inequalities in Eqs. (17) and (19) were previously derived in [12], but we restate them again under the view of the Fourier Transforms and to provide uniformity to our reasoning line.

The bandwidth of a linearly-modulated digital signal is determined by the transmit pulse-shaping filter $g_T(t)$ (see Fig. 1). A suitable solution to minimize the Inter-Symbol Interference (ISI) is the raised cosine filter [25]

$$G_T(f) = \begin{cases} T_s & |f| < f_1 \\ \dfrac{T_s}{2}\left[1+\cos\left(\dfrac{\pi(|f|-f_1)}{\frac{1}{T_s}-2f_1}\right)\right] & f_1 \leq |f| \leq f_2 \\ 0 & |f| > f_2, \end{cases} \tag{20}$$

with $f_1 = (1-\rho)/(2T_s)$; $f_2 = (1+\rho)/(2T_s)$; $\rho \in [0,1]$ is the roll-off factor which determines the smoothness of its frequency response. The signal bandwidth is given by [25]

$$B = \frac{1+\rho}{T_s} \text{ [Hz]}, \quad \text{with } B = \frac{B_\omega}{2\pi}. \tag{21}$$

When restriction (19) is expressed in terms of the TMA period, we have $(1/T_0) > B$, which together with (21) leads to

$$T_0 < \frac{T_s}{1+\rho} \quad \textbf{(restriction 2)}. \tag{22}$$

According to the scheme in Fig. 1, if the bit rate at the input of the symbol mapper is $R_b = J/T_s$ bit/s (with J being the number of bits per symbol) and (21) is taken into account, the

modulation spectral efficiency is given by

$$\frac{R_b}{B} = \frac{J/T_s}{B} = \frac{J}{1+\rho} = \frac{\log_2 M}{1+\rho} \text{ [(bit/s)/Hz]}, \tag{23}$$

which reveals that the spectral efficiency is maximized when ρ takes small values and/or the alphabet order, M, is large.

Let us now analyze, in the time domain, the effects of a TMA on the transmission of a linearly modulated digital signal. Substituting (2) into (9), the signal transmitted by the n-th antenna element can be rewritten as

$$\tilde{s}_n(\theta,t) = \left[\sqrt{2}u(t)\sum_{q=-\infty}^{\infty} G_{nq}\mathrm{e}^{jq\omega_0 t} I_n \mathrm{e}^{jkz_n\cos\theta}\right]\mathrm{e}^{j\omega_c t}. \tag{24}$$

Again, the expression of the radiated signal in the time domain corresponds to the contribution of the N elements

$$\begin{aligned}\tilde{s}_{\text{rad}}(\theta,t) &= \sum_{n=0}^{N-1}\tilde{s}_n(\theta,t)\\ &= \left[\sqrt{2}u(t)\sum_{n=0}^{N-1}\sum_{q=-\infty}^{\infty} G_{nq} I_n \mathrm{e}^{jkz_n\cos\theta}\right]\mathrm{e}^{j(\omega_c+q\omega_0)t}.\end{aligned} \tag{25}$$

In view of (25), it is immediate the need of the first restriction (17) in order to avoid the interference between the carrier and the fundamental frequency of the array pulse modulation. At the same time, the second restriction (22) is also mandatory in order that the unwanted harmonics outside the bandwidth of the information signal $u(t)$ be filtered out.

Recall that the desired signal is the one corresponding to $q = 0$, which is given by

$$\tilde{s}_{\text{rad}}(\theta,t)\Big|_{q=0} = \sqrt{2}u(t)\left[\sum_{n=0}^{N-1} I_n G_{n0}\mathrm{e}^{jkz_n\cos\theta}\right]\mathrm{e}^{j\omega_c t}. \tag{26}$$

From the equation above we are able to ensure that, under restrictions (17) and (22), such a signal could be processed at the receiver as a conventional linearly modulated digital signal so that after I/Q demodulation, low-pass filtering and detection, the transmitted symbols would be properly recovered.

III. Analysis of the Radiated Power

Our aim in this section is to obtain the total power radiated by the TMA when a linearly modulated digital signal is transmitted. We will start by considering the analysis of the signal time-varying power, making use of the mean power density concept. Then we will continue

with the analogous density function considered in the frequency domain, and built on Parseval's identity. Although both analysis will lead to the same results, we will see that the paths followed in each case will enlighten some different, yet complementary, features.

A. Analysis of the Radiated Power: Time Domain

Since the real part of the radiated signal (10) ultimately represents the real-valued magnitude of the electric field vector in the far region of the antenna array, its square will be a real-valued number proportional to the magnitude of the Poynting's vector[1], which will represent the power density (measured in W/m^2) of the signal evaluated at the angular point θ and at time t. The power (spatial) density averaged over time will consequently be

$$\mathcal{D}_{\text{rad}}(\theta) = \lim_{\mathcal{T}\to\infty} \frac{1}{\mathcal{T}} \int_{-\mathcal{T}/2}^{\mathcal{T}/2} s_{\text{rad}}^2(\theta,t)dt \quad \left[\frac{\text{W}}{\text{m}^2}\right]. \tag{27}$$

By considering (9) and (10), we can write

$$\begin{aligned} s_{\text{rad}}(\theta,t) &= \text{Re}\left\{\tilde{s}_{\text{rad}}(\theta,t)\right\} = \text{Re}\left\{\sum_{n=0}^{N-1} \tilde{s}_n(\theta,t)\right\} \\ &= \text{Re}\left\{\sum_{n=0}^{N-1} r_n(\theta,t)\text{e}^{j\omega_c t}\right\}. \end{aligned} \tag{28}$$

For a clearer analysis, we can express the above as

$$\begin{aligned} s_{\text{rad}}(\theta,t) &= \text{Re}\left\{|r(\theta,t)|\,\text{e}^{j\psi(t)}\text{e}^{j\omega_c t}\right\} \\ &= |r(\theta,t)|\cos\left(\omega_c t + \psi(t)\right), \text{ where} \end{aligned} \tag{29}$$

$$r(\theta,t) = \sum_{n=0}^{N-1} r_n(\theta,t) = |r(\theta,t)|\text{e}^{j\psi(t)} \tag{30}$$

is the complex envelope of $s_{\text{rad}}(\theta,t)$ –and thus $|r(\theta,t)|$ represents the real-valued envelope of $s_{\text{rad}}(\theta,t)$.

[1]We can depart from the Poynting's (real-valued) vector $\vec{P}_v = \mu_0^{-1}\vec{E}\times\vec{B}$ (μ_0 is the vacuum magnetic permeability). Since at far distances from the antenna $\vec{E}$ and $\vec{B}$ are perpendicular to each other and their magnitudes satisfy the relationship $E = cB$ –being c the speed of light in vacuum–, then $\vec{P}_v = (\mu_0 c)^{-1}E^2\vec{k}$, where $\vec{k}$ is the wave vector pointing in the direction of the advancing electromagnetic plane wave. Finally, $P_v \propto E^2$, i.e. $P_v \propto s_{\text{rad}}^2(\theta,t)$. By adjusting the constant of proportionality to be equal to one, we can obtain a quantity which is measured in W/m^2, as indicated in (27).

Substituting (29) into (27), and taking into account that $\cos^2(x) = [1 + \cos(2x)]/2$, we have

$$\mathcal{D}_{\text{rad}}(\theta) = \frac{1}{2} \lim_{\mathcal{T}\to\infty} \frac{1}{\mathcal{T}} \int_{-\mathcal{T}/2}^{\mathcal{T}/2} |r(\theta,t)|^2 dt + \\ + \frac{1}{2} \lim_{\mathcal{T}\to\infty} \frac{1}{\mathcal{T}} \int_{-\mathcal{T}/2}^{\mathcal{T}/2} |r(\theta,t)|^2 \cos\left(2\omega_c t + 2\psi(t)\right) dt. \tag{31}$$

In view of (9) and (30), and considering restrictions (17) and (22), we can conclude that the real-valued envelope $|r(\theta,t)|^2$ varies slowly relative to the rapid variations (twice the carrier frequency plus slow variations in phase due to $2\psi(t)$) of the cosine function. Then the net area contributed by the right-hand-side integral in (31) is very small compared to the value of the left-hand-side term and, hence, it can be neglected [25]. We can then safely write

$$\mathcal{D}_{\text{rad}}(\theta) = \frac{1}{2} \lim_{\mathcal{T}\to\infty} \frac{1}{\mathcal{T}} \int_{-\mathcal{T}/2}^{\mathcal{T}/2} |r(\theta,t)|^2 dt. \tag{32}$$

We now develop the integrand. From (30) we find that

$$\begin{aligned} |r(\theta,t)|^2 &= r(\theta,t) r^*(\theta,t) \\ &= \sum_{n=0}^{N-1} |r_n(\theta,t)|^2 + \sum_{n=0}^{N-1} \sum_{\substack{m=0 \\ m\neq n}}^{N-1} r_n(\theta,t) r_m^*(\theta,t), \end{aligned} \tag{33}$$

but with the help of (9) and (2) the sum over the squared amplitude terms becomes

$$\begin{aligned} \sum_{n=0}^{N-1} |r_n(\theta,t)|^2 &= 2 \sum_{n=0}^{N-1} |I_n|^2 |u(t)|^2 |g_n(t)|^2 \\ &= 2 \sum_{n=0}^{N-1} |I_n|^2 |u(t)|^2 \left[\sum_{q=-\infty}^{\infty} G_{nq} \mathrm{e}^{jq\omega_0 t} \sum_{p=-\infty}^{\infty} G_{np}^* \mathrm{e}^{-jp\omega_0 t} \right] \\ &= 2 \sum_{n=0}^{N-1} |I_n|^2 \left[\sum_{q=-\infty}^{\infty} |G_{nq}|^2 + \right. \\ &\quad \left. + \sum_{p=-\infty}^{\infty} \sum_{\substack{q=-\infty \\ q\neq p}}^{\infty} G_{np} G_{nq}^* \mathrm{e}^{j(p-q)\omega_0 t} \right] |u(t)|^2, \end{aligned} \tag{34}$$

whereas

$$\sum_{m=0}^{N-1}\sum_{\substack{n=0\\n\neq m}}^{N-1} r_m(\theta,t)r_n^*(\theta,t) =$$

$$2\sum_{m=0}^{N-1}\sum_{\substack{n=0\\n\neq m}}^{N-1} |u(t)|^2 I_m I_n^* \mathrm{e}^{jk(z_m-z_n)\cos\theta}\cdot$$

$$\cdot\left[\sum_{q=-\infty}^{\infty} G_{mq}\mathrm{e}^{jq\omega_0 t}\cdot\sum_{p=-\infty}^{\infty} G_{np}^*\mathrm{e}^{-jp\omega_0 t}\right]$$

$$= 2\sum_{m=0}^{N-1}\sum_{\substack{n=0\\n\neq m}}^{N-1} I_m I_n^*\mathrm{e}^{jk(z_m-z_n)\cos\theta}\left[\sum_{q=-\infty}^{\infty} G_{mq}G_{nq}^* + \right.$$

$$\left. + \sum_{p=-\infty}^{\infty}\sum_{\substack{q=-\infty\\q\neq p}}^{\infty} G_{mp}G_{nq}^*\mathrm{e}^{j(p-q)\omega_0 t}\right]|u(t)|^2. \tag{35}$$

On the other hand, if we consider the integral

$$I = \int_{-\infty}^{\infty} |u(t)|^2\mathrm{e}^{-j(q-p)\omega_0 t}dt, \tag{36}$$

with $p \neq q$, we can see that it coincides with $\mathrm{FT}\left[|u(t)|^2\right]$ evaluated at a non-zero integer multiple of ω_0 frequency. As a consequence of the convolution property (12)[2], $\mathrm{FT}\left[|u(t)|^2\right]$ has a bandwidth equal to B_ω. Therefore, it does not have any components at frequencies away from the $[-B_\omega, B_\omega]$ range. Under restriction (19) the integral I then vanishes.

If we substitute Eqs. (34) and (35) into (33), and then integrate (32) considering that the integral (36) is equal to zero, we arrive at

$$\mathcal{D}_{\text{rad}}(\theta) = \sum_{q=-\infty}^{\infty}\left[\sum_{n=0}^{N-1}|I_n|^2|G_{nq}|^2 + \right.$$

$$\left. + \sum_{m=0}^{N-1}\sum_{\substack{n=0\\n\neq m}}^{N-1} I_m I_n^* G_{mq}G_{nq}^*\mathrm{e}^{jk(z_m-z_n)\cos\theta}\right]\cdot\mathcal{D}_u, \tag{37}$$

[2]The frequency range of $U(\omega)$ and $U(-\omega)$ is $[-B_\omega/2, B_\omega/2]$, determined by $G_T = \mathrm{FT}[g_T(t)]$ (see (20)). $\mathrm{FT}\left\{|u(t)|^2\right\} = \mathrm{FT}\left\{u(t)u^*(t)\right\} = \frac{1}{2\pi}U(\omega)\star U^*(-\omega)$, whose frequency range can be easily deduced from the convolution properties, yielding $[-B_\omega, B_\omega]$.

where

$$\mathcal{D}_u = \mathcal{D}_s = \lim_{\mathcal{T}\to\infty} \frac{1}{\mathcal{T}} \int_{-\mathcal{T}/2}^{\mathcal{T}/2} |u(t)|^2 dt \tag{38}$$

is referred to isotropic elements. Therefore it is constant with respect to the spatial coordinates (the dependency is not explicitly shown) and represents the baseband-equivalent signal mean power density which, as a matter of fact, equals the baseband counterpart. Let us show this last point. To compute the mean power density of $s(t)$ as defined in (4) we have to take the integral of $s^2(t)$:

$$\begin{aligned}
\mathcal{D}_s &= \lim_{\mathcal{T}\to\infty} \frac{1}{\mathcal{T}} \int_{-\mathcal{T}/2}^{\mathcal{T}/2} s^2(t) dt \\
&= \lim_{\mathcal{T}\to\infty} \frac{1}{\mathcal{T}} \int_{-\mathcal{T}/2}^{\mathcal{T}/2} 2A^2(t) \cos^2\left(\omega_c t + \alpha(t)\right) dt \\
&= \lim_{\mathcal{T}\to\infty} \frac{1}{\mathcal{T}} \int_{-\mathcal{T}/2}^{\mathcal{T}/2} |u(t)|^2 dt = \mathcal{D}_u,
\end{aligned} \tag{39}$$

with $|u(t)| = A(t)$, and where the first three equalities were obtained by reasoning analogously to the steps from (27) to (32). The last identity was obtained from the definition of the mean power of a complex-valued signal [25][3].

The total mean power P_{rad} is computed by integrating $\mathcal{D}_{\text{rad}}$ over a sphere of constant large (far field) radius[4], i.e.

$$\begin{aligned}
P_{\text{rad}} &= \int_0^{2\pi} \int_0^{\pi} \mathcal{D}_{\text{rad}}(\theta) \sin(\theta) d\theta d\varphi \\
&= 2\pi \int_0^{\pi} \mathcal{D}_{\text{rad}}(\theta) \sin(\theta) d\theta \qquad [\text{W}].
\end{aligned} \tag{40}$$

[3]The equivalent baseband signal $u(t)$ is defined in (5) as the superposition of two orthogonal signals $a(t)$ and $b(t)$ satisfying: $\int_{-\infty}^{\infty} a(t)b(t)dt = 0$. The power of $u(t)$ will be given by: $P_u = \lim_{\mathcal{T}\to\infty} \frac{1}{\mathcal{T}} \int_{-\mathcal{T}/2}^{\mathcal{T}/2} \left(a(t) + b(t)\right)^2 dt = \lim_{\mathcal{T}\to\infty} \frac{1}{\mathcal{T}} \int_{-\mathcal{T}/2}^{\mathcal{T}/2} \left(a^2(t) + b^2(t)\right) dt = \lim_{\mathcal{T}\to\infty} \frac{1}{\mathcal{T}} \int_{-\mathcal{T}/2}^{\mathcal{T}/2} |u(t)|^2 dt$.

[4]Notice that the implicit factor $\mathrm{e}^{j\vec{k}\cdot\vec{R}}/R$, being $\vec{R}$ the field point vector, in the array factor (1) allows us to assign W/m^2 units to both $\mathcal{D}_u$ and $\mathcal{D}_{\text{rad}}$.

Since $\int_0^\pi \mathrm{e}^{jK\cos\theta}\sin\theta d\theta = 2\,\mathrm{sinc}(K)$, we obtain:

$$P_{\text{rad}} = \sum_{q=-\infty}^{\infty}\left[\sum_{n=0}^{N-1}|I_n|^2|G_{nq}|^2 + \right.$$
$$\left.\sum_{m=0}^{N-1}\sum_{\substack{n=0\\n\neq m}}^{N-1} I_m I_n^* G_{mq} G_{nq}^* \,\mathrm{sinc}(k(z_m - z_n))\right] 4\pi\mathcal{D}_u. \tag{41}$$

Note that we can associate every couple of summands in

$$\sum_{m=0}^{N-1}\sum_{\substack{n=0\\n\neq m}}^{N-1} I_m I_n^* G_{mq} G_{nq}^* \,\mathrm{sinc}(k(z_m - z_n)),$$

which have crossed m and n indexes as illustrated below:

$$\begin{aligned} &I_m I_n^* G_{mq} G_{nq}^* \,\mathrm{sinc}(k(z_m - z_n)) + \\ &+ I_n I_m^* G_{nq} G_{mq}^* \,\mathrm{sinc}(k(z_n - z_m)) \\ &= 2\,\mathrm{Re}\{I_m I_n^* G_{mq} G_{nq}^*\}\,\mathrm{sinc}(k(z_m - z_n)). \end{aligned}$$

Since sinc is an even function, the first term above is the complex conjugate of the second one and the sum leads to a real value. Therefore, we can simplify (41) yielding:

$$P_{\text{rad}} = \sum_{q=-\infty}^{\infty}\left[\sum_{n=0}^{N-1}|I_n|^2|G_{nq}|^2 + \right.$$
$$\left.2\sum_{m=0}^{N-1}\sum_{\substack{n=0\\n\neq m}}^{N-1} \mathrm{Re}\{I_m I_n^* G_{mq} G_{nq}^*\}\,\mathrm{sinc}(k(z_m - z_n))\right] \cdot$$
$$\cdot\, 4\pi\mathcal{D}_u = \mathcal{G}_{\text{TMA}} P_{u\text{i}}, \tag{42}$$

where $P_{u\text{i}} = 4\pi\mathcal{D}_u$ (measured in W) represents the power radiated by an isotropic antenna transmitting a linearly modulated equivalent baseband digital signal $u(t) \in \mathbb{C}$ with a power density $\mathcal{D}_u$, whereas $\mathcal{G}_{\text{TMA}}$ represents the TMA power transfer function (dimensionless) accounting for both the array geometry and the time-modulated elements radiating a carrier signal. The $\mathcal{G}_{\text{TMA}}$ expression coincides with the array total power in [12, Eq. (30)] and, as expressed there, such

a factor can be used to separate the useful power ($q = 0$) from the harmonic SR ($q \neq 0$) losses in a similar way than that described in this work. By splitting up those terms we have

$$P_{\text{rad}} = \left(\mathcal{G}_{\text{TMA}_0} + \mathcal{G}_{\text{TMA}_{\text{SR}}}\right) P_{ui}, \tag{43}$$

where $\mathcal{G}_{\text{TMA}_0} = \mathcal{G}_{\text{TMA}}\Big|_{q=0}$ and $\mathcal{G}_{\text{TMA}_{\text{SR}}} = \mathcal{G}_{\text{TMA}}\Big|_{q\neq 0}$.

B. Analysis of the Radiated Power: Frequency Domain

The power radiated density in the frequency domain can be found by applying Parseval's theorem [24], [25] to (27):

$$\mathcal{D}_{\text{rad}}(\theta) = \frac{1}{2\pi} \lim_{\mathcal{W}\to\infty} \frac{1}{\mathcal{W}} \int_{-\mathcal{W}/2}^{\mathcal{W}/2} |S_{\text{rad}}(\theta,\omega)|^2 d\omega, \tag{44}$$

where $|S_{\text{rad}}(\theta,\omega)|^2 = |\text{FT}\left[s_{\text{rad}}(\theta,t)\right]|^2$ is the energy spectral density of the signal transmitted by the array that is a function of both angular spherical coordinates and frequency.

By considering the relationship between the radiated signal (28) and its complex-valued representation (10)

$$s_{\text{rad}}(\theta,t) = \text{Re}\left\{\tilde{s}_{\text{rad}}(\theta,t)\right\} = \left(\tilde{s}_{\text{rad}}(\theta,t) + \tilde{s}^*_{\text{rad}}(\theta,t)\right)/2, \tag{45}$$

and applying the FT we obtain

$$S_{\text{rad}}(\theta,\omega) = \left(\tilde{S}_{\text{rad}}(\theta,\omega) + \tilde{S}^*_{\text{rad}}(\theta,-\omega)\right)/2. \tag{46}$$

Taking Eqs. (15), (17) and (22) into account we can obtain[5]

$$|S_{\text{rad}}(\theta,\omega)|^2 = \frac{1}{4}\left[|\tilde{S}_{\text{rad}}(\theta,\omega)|^2 + |\tilde{S}_{\text{rad}}(\theta,-\omega)|^2\right]. \tag{47}$$

[5]In the expansion $|S_{\text{rad}}(\theta,\omega)|^2 = \frac{1}{4}\{\tilde{S}_{\text{rad}}(\theta,\omega)\tilde{S}^*_{\text{rad}}(\theta,\omega)$
$+\tilde{S}_{\text{rad}}(\theta,\omega)\tilde{S}_{\text{rad}}(\theta,-\omega) + \tilde{S}^*_{\text{rad}}(\theta,-\omega)\tilde{S}^*_{\text{rad}}(\theta,\omega) + \tilde{S}^*_{\text{rad}}(\theta,-\omega)\tilde{S}_{\text{rad}}(\theta,-\omega)\}$
the terms $\tilde{S}_{\text{rad}}(\theta,\omega)\tilde{S}_{\text{rad}}(\theta,-\omega)$ and $\tilde{S}^*_{\text{rad}}(\theta,-\omega)\tilde{S}^*_{\text{rad}}(\theta,\omega)$ will vanish. This is readily seen with the help of Fig. 2: $|\tilde{S}_{\text{rad}}(\theta,\omega)|$ is centered at ω_c, so $|\tilde{S}_{\text{rad}}(\theta,-\omega)|$ will be centered at $-\omega_c$ (because $|\tilde{S}_{\text{rad}}(\theta,-\omega)|$ will be obtained by reflecting $|\tilde{S}_{\text{rad}}(\theta,\omega)|$ with respect to the $\omega = 0$ axis). Thus, the larger amplitudes of $\tilde{S}_{\text{rad}}(\theta,\omega)$ (i.e., ω around ω_c) will fall into the region where $|\tilde{S}_{\text{rad}}(\theta,-\omega)|$ is zero (due to the fact that $\omega_c \gg \omega_0$ (see (17) and comments below (3)), and vice versa, the relevant nonzero values of $|\tilde{S}_{\text{rad}}(\theta,-\omega)|$ will fall into the regions where $|\tilde{S}_{\text{rad}}(\theta,\omega)|$ is zero. Therefore, their multiplication will be zero for $-\infty < \omega < \infty$. The same reasoning applies to the other product. Besides, $|\tilde{S}^*_{\text{rad}}(\theta,-\omega)|^2 = |\tilde{S}_{\text{rad}}(\theta,-\omega)|^2$.

Substituting (47) into (44) we have

$$\frac{1}{2\pi}\lim_{\mathcal{W}\to\infty}\frac{1}{\mathcal{W}}\int_{-\mathcal{W}/2}^{\mathcal{W}/2}\frac{1}{4}\left[|\tilde{S}_{\text{rad}}(\theta,\omega)|^2+|\tilde{S}_{\text{rad}}(\theta,-\omega)|^2\right]d\omega$$
$$=\frac{1}{4\pi}\lim_{\mathcal{W}\to\infty}\frac{1}{\mathcal{W}}\int_{-\mathcal{W}/2}^{\mathcal{W}/2}|\tilde{S}_{\text{rad}}(\theta,\omega)|^2d\omega=\mathcal{D}_{\text{rad}}(\theta). \tag{48}$$

We now calculate

$$|\tilde{S}_{\text{rad}}(\theta,\omega)|^2=\left[\sum_{n=0}^{N-1}\tilde{S}_n(\theta,\omega)\right]\left[\sum_{n=0}^{N-1}\tilde{S}_n^*(\theta,\omega)\right]$$
$$=\sum_{n=0}^{N-1}|\tilde{S}_n(\theta,\omega)|^2+\sum_{m=0}^{N-1}\sum_{\substack{n=0\\n\neq m}}^{N-1}\tilde{S}_m(\theta,\omega)\tilde{S}_n^*(\theta,\omega). \tag{49}$$

The two sums above are easily determined from (15) and restrictions (17) and (19). Indeed,

$$\sum_{n=0}^{N-1}|\tilde{S}_n(\theta,\omega)|^2=\sum_{n=0}^{N-1}\left[\sum_{q=-\infty}^{\infty}|I_n|^2|G_{nq}|^2V(\omega,q)\right], \tag{50}$$

and

$$\sum_{m=0}^{N-1}\sum_{\substack{n=0\\n\neq m}}^{N-1}\tilde{S}_m(\theta,\omega)\tilde{S}_n^*(\theta,\omega)=$$
$$\sum_{m=0}^{N-1}\sum_{\substack{n=0\\n\neq m}}^{N-1}\sum_{q=-\infty}^{\infty}I_mI_n^*G_{mq}G_{nq}^*\mathrm{e}^{jk(z_m-z_n)\cos\theta}V(\omega,q), \tag{51}$$

where $V(\omega,q)=2|U(\omega-(\omega_c+q\omega_0))|^2$. Substituting Eqs. (50) and (51) in (49), and the result in the integral (44) we have:

$$\mathcal{D}_{\text{rad}}(\theta)=\frac{1}{4\pi}\lim_{\mathcal{W}\to\infty}\frac{1}{\mathcal{W}}\int_{-\mathcal{W}/2}^{\mathcal{W}/2}\sum_{q=-\infty}^{\infty}\left[\sum_{n=0}^{N-1}|I_n|^2|G_{nq}|^2+\right.$$
$$\left.\sum_{m=0}^{N-1}\sum_{\substack{n=0\\n\neq m}}^{N-1}I_mI_n^*G_{mq}G_{nq}^*\mathrm{e}^{jk(z_m-z_n)\cos\theta}\right]V(\omega,q)d\omega. \tag{52}$$

For each index q, we must solve:

$$\frac{1}{2\pi}\lim_{\mathcal{W}\to\infty}\frac{1}{\mathcal{W}}\int_{-\mathcal{W}2}^{\mathcal{W}/2}|U(\omega-(\omega_c+q\omega_0))|^2d\omega$$
$$=\frac{1}{2\pi}\lim_{\mathcal{W}\to\infty}\frac{1}{\mathcal{W}}\int_{-\mathcal{W}/2}^{\mathcal{W}/2}|U(\omega)|^2d\omega$$
$$=\frac{1}{2\pi}\lim_{\mathcal{W}\to\infty}\frac{1}{\mathcal{W}}\int_{-\mathcal{W}/2}^{\mathcal{W}/2}|S(\omega)|^2d\omega=\mathcal{D}_S=\mathcal{D}_U, \tag{53}$$

where $\mathcal{D}_S = \mathcal{D}_U$ is the power density of the linearly modulated digital signal. By considering Parseval's theorem in (39), the equality $\mathcal{D}_U = \mathcal{D}_u$ is satisfied. Also, the first equality in (53) is true because, according to restrictions in Eqs. (17) and (22), signals inside the respective integrals in (52) (independently of q) are replicas of $|U(\omega)|^2$. Consequently, each of the areas under them over their respective frequency range for a given q is exactly the same as the one centered at the origin. Furthermore, according to Eqs. (5) and (7), $u(t)$ is given by

$$u(t) = \sum_{k=-\infty}^{\infty} c_k g_T(t - kT_s), \tag{54}$$

where $c_k = a_k + jb_k$ are complex-valued symbols. Hence, $u(t)$ is an infinite sequence of symbols which we will assume zero-mean and uncorrelated. Recall that every T_s seconds we send a pulse of the form $c_k g_T(t-kT_s)$ with an average energy spectral density $E_s|G_T(\omega/2\pi)|^2 = E_s|G_T(f)|^2$, with E_s being the average symbol energy of the sequence. Therefore, the power spectral density of $u(t)$ is obtained as $E_s|G_T(f)|^2/T_s$. Consequently, the integral in (53) in terms of the energy spectral density of $u(t)$ can be expressed as

$$\mathcal{D}_U = \frac{1}{2\pi} \lim_{\mathcal{W}\to\infty} \int_{-\mathcal{W}/2}^{\mathcal{W}/2} \frac{E_s|G_T(\omega/2\pi)|^2}{T_s} d\omega = \frac{E_s\|g_T\|^2}{T_s}, \tag{55}$$

where $\|g_T\|^2$ is the energy of the shaping pulse in (20):

$$\|g_T\|^2 = \frac{1}{2\pi} \lim_{\mathcal{W}\to\infty} \int_{-\mathcal{W}/2}^{\mathcal{W}/2} |G_T(\omega/2\pi)|^2 d\omega = \frac{T_s(4-\rho)}{4}, \tag{56}$$

which leads to a simple expression for $\mathcal{D}_U$:

$$\mathcal{D}_U = \left(E_s(4-\rho)\right)/4. \tag{57}$$

Therefore, by considering (53) and the equality $\mathcal{D}_U = \mathcal{D}_u$, (52) takes exactly the form of (37). Then, by integrating (52) over the whole space according to (40), and taking into account the definition of $\mathcal{G}_{\text{TMA}}$ in (42) we arrive to

$$P_{\text{rad}} = \mathcal{G}_{\text{TMA}} 4\pi \mathcal{D}_U = \mathcal{G}_{\text{TMA}} P_{ui} \quad [\text{W}], \tag{58}$$

which is, as expected, the same result as that given in (42).

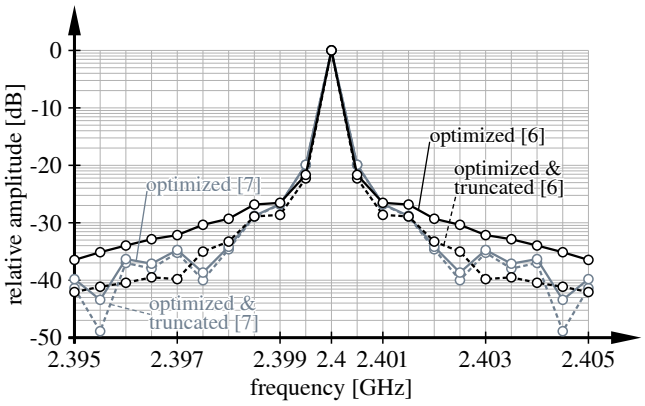

Fig. 3. TMA total mean normalized radiated power (mapping the first $\mathcal{G}_{\text{TMA}}$ meaningful terms) for the example in Section IV.

IV. EXAMPLE

As a numerical example we consider two TMAs optimized through Simulated Annealing (SA) and published in [6, Fig. 2] and [7, Table 3]. We also consider –without impact in terms of maximum Side-lobe Level (SLL) of the $q = 0$ power pattern– an inter-element distance $d = \lambda/2$ (instead of $d = 0.7\lambda$ used in [6], [7]). Both TMAs transmit a M-QAM signal with $M = 256$ and $R_b = 1\,\text{Mbit/s}$. Given that $R_b = J/T_s$, with $J = log_2(M) = 8$, the symbol period is $T_s = J/R_b = 8\,\mu\text{s}$. The modulator has a shaping filter with $\rho = 0.2$, yielding a signal bandwidth $B = (1+\rho)/T_s = 150\,\text{kHz}$ according to (21).

We plot in Fig. 3 the distribution of the total mean normalized radiated power at the carrier frequency $f_c = 2.4\,\text{GHz}$ and at the first ten multiples of $f_0 = 500\,\text{kHz}$, i.e. the mapping of the corresponding terms of the $\mathcal{G}_{\text{TMA}}$ defined in (42). The curves labeled as "optimized" corresponds directly to the above-mentioned pulse distribution, while "optimized & truncated" curves consider permanently in off-state those elements whose normalized pulse durations are very close to zero (elements 1, 3, 4, and 5 in [6]), while those elements whose normalized pulse durations are very close to one (elements 23 and 29 in [6]; and elements 14 and 15 in [7]) are set permanently to on-state. The TMA power efficiency [12] is improved from 96.7 % to 98 % for [6] (lowering the overall SR level), and from 96.8 % to 97 % for [7], keeping the main ($q = 0$) power pattern SLL topology almost unchanged (for [6], the maximum SLL equals -20.02 dB for the non truncated case, and -19.43 dB for the truncated one; -15.91 dB and -15.90 dB for [7], respectively).

V. Conclusion

The possible impact on the information content caused by TMAs when used for transmission of linearly modulated signals can be overridden if constraints in Eqs. (17) and (22) are applied. Under those conditions, together with the assumption of a fast decaying rate of the harmonics level as a function of q, a generalized TMA power response is accurately derived and given by the product of its power transfer function and the equivalent baseband signal power. The TMA transfer power function is presented as its canonical response. In other words, the TMA radiated power when a single carrier at its center-frequency is transmitted.

Both time and frequency domain analyses have been carried out to quantify the power-radiated efficiency of the TMA when it is combined with digital linear modulation schemes, hence allowing for the use of conditioned TMAs in wireless communication systems.

Acknowledgment

This work has been funded by Xunta de Galicia, MINECO of Spain, and FEDER funds of the EU under grants 2012/287, IPT-2011-1034-370000, TEC2010-19545-C04-01, and CSD2008-00010.

References

[1] W. Kummer, A. Villeneuve, T. Fong, and F. Terrio, "Ultra-low sidelobes from time-modulated arrays," *IEEE Trans. Antennas Propag.*, vol. 11, no. 6, pp. 633–639, 1963.

[2] S. Yang, Y.-B. Gan, and A. Qing, "Sideband suppression in time-modulated linear arrays by the differential evolution algorithm," *IEEE Antennas Wireless Propag. Lett.*, vol. 1, no. 1, pp. 173–175, 2002.

[3] S. Yang, Y.-B. Gan, and T. Peng Khiang, "A new technique for power-pattern synthesis in time-modulated linear arrays," *IEEE Antennas and Wireless Propagation Letters*, vol. 2, no. 1, pp. 285–287, 2003.

[4] S. Yang, Y.-B. Gan, and P. K. Tan, "Linear antenna arrays with bidirectional phase center motion," *IEEE Trans. Antennas Propag.*, vol. 53, no. 5, pp. 1829–1835, 2005.

[5] S. Yang, Y.-B. Gan, A. Qing, and P. K. Tan, "Design of a uniform amplitude time modulated linear array with optimized time sequences," *IEEE Trans. Antennas Propag.*, vol. 53, no. 7, pp. 2337–2339, 2005.

[6] J. Fondevila, J. Bregains, F. Ares, and E. Moreno, "Optimizing uniformly excited linear arrays through time modulation," *IEEE Antennas and Wireless Propagation Letters*, vol. 3, no. 1, pp. 298–301, 2004.

[7] ——, "Application of time modulation in the synthesis of sum and difference patterns by using linear arrays," *Microw. Opt. Technol. Lett.*, vol. 48, p. 829–832, 2006.

[8] L. Poli, P. Rocca, L. Manica, and A. Massa, "Handling sideband radiations in time-modulated arrays through particle swarm optimization," *IEEE Trans. Antennas Propag.*, vol. 58, no. 4, 2010.

[9] A. Tennant and B. Chambers, "Control of the harmonic radiation patterns of time-modulated antenna arrays," in *Proc. of IEEE Antennas and Propag. Society Int. Symposium (AP-S 2008)*, 2008, pp. 1–4.

[10] E. Aksoy and E. Afacan, "Generalized representation of sideband radiationpower calculation in arbitrarily distributed time-modulated planar and linear arrays," in *Progress in Electromagnetics Research Symposium (PIERS 2011)*, Suzhou, China, Sep. 2011, pp. 368–371.

[11] L. Poli, P. Rocca, L. Manica, and A. Massa, "Pattern synthesis in time-modulated linear arrays through pulse shifting," *IET Microwaves, Antennas Propagation*, vol. 4, no. 9, pp. 1157–1164, 2010.

[12] J. Bregains, J. Fondevila-Gomez, G. Franceschetti, and F. Ares, "Signal radiation and power losses of time-modulated arrays," *IEEE Trans. Antennas Propag.*, vol. 56, no. 6, pp. 1799–1804, 2008.

[13] E. Aksoy and E. Afacan, "Calculation of sideband power radiation in time-modulated arrays with asymmetrically positioned pulses," *IEEE Antennas and Wireless Propagation Letters*, vol. 11, pp. 133–136, 2012.

[14] S. Yang, Y. Gan, and P. Tan, "Evaluation of directivity and gain for time-modulated linear antenna arrays," *Microw. Opt. Technol. Lett.*, vol. 42, p. 167–171, 2004.

[15] L. Poli, P. Rocca, L. Manica, and A. Massa, "Time modulated planar arrays - analysis and optimisation of the sideband radiations," *IET Microwaves, Antennas Propagation*, vol. 4, no. 9, pp. 1165–1171, Sep. 2010.

[16] P. Rocca, L. Poli, G. Oliveri, and A. Massa, "Adaptive nulling in time-varying scenarios through time-modulated linear arrays," *IEEE Antennas and Wireless Propagation Letters*, vol. 11, pp. 101–104, 2012.

[17] L. Poli, P. Rocca, G. Oliveri, and A. Massa, "Harmonic beamforming in time-modulated linear arrays," *IEEE Trans. Antennas Propag.*, vol. 59, no. 7, pp. 2538–2545, Jul. 2011.

[18] G. Li, S. Yang, Y. Chen, and Z. Nie, "A hybrid analog-digital adaptive beamforming in time-modulated linear arrays," *Electromagnetics*, vol. 30, no. 4, 2010.

[19] G. Li, S. Yang, Y. Chen, and Z.-P. Nie, "A novel electronic beam steering technique in time modulated antenna array," *Progress In Electromagnetics Research*, vol. 97, pp. 391–405, 2009.

[20] G. Li, S. Yang, and Z. Nie, "Direction of arrival estimation in time modulated linear arrays with unidirectional phase center motion," *IEEE Trans. Antennas Propag.*, vol. 58, no. 4, pp. 1105—-1111, Apr. 2010.

[21] G. Li, S. Yang, Z. Zhao, and Z.-P. Nie, "A study of AM and FM signal reception of time modulated linear antenna arrays," *Progress In Electromagnetics Research Letters*, vol. 7, pp. 171–181, 2009.

[22] Q. Zhu, S. Yang, R. Yao, M. Huang, and Z. Nie, "Unified time- and frequency-domain study on time-modulated arrays," *IEEE Trans. Antennas Propag.*, vol. 61, no. 6, pp. 3069–3076, Jun. 2013.

[23] Q. Zhu, S. Yang, R. Yao, and Z. Nie, "Directional modulation based on 4-D antenna arrays," *IEEE Trans. Antennas Propag.*, vol. 62, no. 2, Feb. 2014.

[24] B. Sklar, *Digital Communications*, 2nd ed. Prentice Hall, 2001.

[25] J. Proakis, *Digital Communications*, 5th ed. McGraw-Hill, 2008.

Roberto Maneiro-Catoira received the Telecommunications Engineering degree from the University of Vigo, Spain, in 1995 and the Master of Information and Telecommunications Technologies for Mobile Networks degree in 2012 from the University of A Coruña, Spain, in 2012. He worked from 1996 to 1997 at Egatel company focused on the Research and Development in the field of TV and Radio digital communications. From 1997 to 2000 he was with Siemens Mobile Networks as GSM access network deployment manager. From 2000 to 2003 he worked at Nortel Networks as UMTS network integration manager. From 2003 he is fully dedicated to teaching Siemens Simatic Programmable Logic Devices as well as mathematics for different levels, both for private and public organisms. Actually he is working towards his Ph.D. about dynamic arrays for digital communications in the Electronic Technology and Communications Group (GTEC) at the University of A Coruña.

Julio C. Brégains received in 2000 the B.S. in Electrical Engineering from the National University of the Northeast, Argentina, and the Industrial Engineering degree from the University of León, Spain, in 2006. In 2007 he obtained with honors a Ph.D. degree in Applied Physics from the University of Santiago de Compostela (USC), Spain. He is currently an Assistant Professor of Electronics at the Department of Electronics and Systems of the School of Informatics, at the University of A Coruña, Spain. He is also currently a member of the Electronic Technology and Communications Group (GTEC), at that department. He has co-authored over 70 international journal and conference papers, having received awards for three of them. His research interests include high-frequency electronics, software development for solving electromagnetic problems, antenna array pattern synthesis and design, and variational problems applied to field theory.

José A. García-Naya was born in A Coruña in 1981. He studied Computer Engineering at the University of A Coruña (UDC), Spain, where he obtained his degree “Ingeniero en Informática” in 2005, and his Ph.D. degree in 2010. Since 2005 he is with the Group of Electronic Technology and Communications (GTEC) at the UDC, where he is currently Associate Professor. Since 2008 he spent several months at the Institute of Telecommunications at the Vienna University of Technology collaborating in the experimental evaluation of mobile communications systems. His research interests are in the field of digital communications, with special emphasis on the experimental evaluation of wireless systems.

Luis Castedo was born in Santiago de Compostela, Spain, in 1966. He received the Ingeniero de Telecomunicación and Doctor Ingeniero de Telecomunicación degrees, both from Polytechnic University of Madrid, Spain, in 1990 and 1993, respectively. From November 1994 to October 2001, he was an Associate professor in the Department of Electronics and Systems at University of A Coruña, Spain, where he is currently Full Professor. He has been chairman of the Department between 2003 and 2009. Luis Castedo is coauthor of more than one hundred papers in peer-reviewed international journals and conferences. He has also been principal researcher in more than thirty research projects funded by public organizations and private companies. His research interests are signal processing and digital communications with special emphasis on blind adaptive filtering, estimation/equalization of MIMO channels, space-time coding and prototyping of digital communication equipments.